Available online at www.sciencedirect.com
SCIENCE DIRECT®
Theoretical Population Biology 64 (2003) 89–99
Theoretical Population Biology
http://www.elsevier.com/locate/ytpbi

Correlative coherence analysis: variation from intrinsic and extrinsic sources in competing populations

Wayne M. Getz*

Department of Environmental Science, Policy and Management, University of California, 201 Wellman Hall, Berkeley, CA 94720-3112, USA

Received 1 June 2002

Abstract

The concept of the correlation between two signals is generalized to the *correlative coherence* of a set of n signals by introducing a Shannon–Weaver-type measure of the entropy of the normalized eigenvalues of the n-dimensional correlation matrix associated with the set of signals. Properties of this measure are stated for canonical cases. The measure is then used to evaluate which subsets of a particular set of n signals are more or less coherent. This set of signals comprises extrinsic, stochastic resource inputs and the population trajectories obtained from simulations of a discrete time model of competing biological populations driven by these resource inputs. The analysis reveals that, at low levels of competition, the correlative coherence of the combined system of intrinsic population and extrinsic resource variables is relatively low, but increases with increasing variation in the resources. Further, at intermediate and high competition levels, the correlative coherence depends more strongly on competition than entrainment of stochasticity in the extrinsic resource variables. Density dependence has the effect of amplifying variation in noise only when this variation is relatively large. Also, chaotic systems appear to be entrained by sufficiently noisy environmental inputs.

Keywords: Correlation matrix; Shannon–Weaver information; Density dependence; Chaos; Time series; Eigenvalues; Entropy

1. Introduction

Temporal variation is invariably evident in biological populations. With regard to the structure of this variation, the relative contributions of extrinsic stochastic forcing functions and intrinsic chaotic dynamics is difficult to distinguish (Cencini et al., 2000). Considerable effort has been made to tease out stochastic noise from a chaotic biological signal (Sugihara et al., 1990; Sugihara and May, 1990; Poon and Barahona, 2001; Bjornstad and Grenfell, 2001). Such analyses also help to reveal the dimension of the underlying deterministic oscillatory or chaotic attractor. In biological populations, this dimension often reflects distinct time-related substructures in the population (e.g. age or stage: see Dennis et al. (2001) in addition to the above references).

Deterministic chaotic dynamics arise in populations that exhibit highly nonlinear density-dependent survival and reproduction rates (May, 1974; May and Oster, 1976; Getz, 1996; Cushing et al., 1998) or in populations that interact among one another in strongly nonlinear ways (Bjornstad et al., 2001). Stochasticity is usually related to environmental variability, although demographic stochasticity becomes important in small populations (Shaffer, 1981). Also, in small populations, the fact that population size is an integer itself impacts the nature of the observed variation (Henson et al., 2001). Finally, observational errors increase the level of stochasticity (or noise) in empirical data.

In addition to considering the degree to which population variation is due to stochastic environmental inputs versus deterministic nonlinearities (cf. Higgins et al., 1997), one can consider the degree to which variation in co-occurring populations is entrained by ecological interactions or common stochastic driving forces. Given that the effects of environmental stochasticity on chaotically varying populations are not well understood (but see Cohen (1995), Kaitala et al. (1997) and Ripa et al. (1998) for analyses of how the frequency spectrum of stochastic processes changes when filtered by density-dependent population processes), the relative effects of stochastic inputs versus population processes

*Fax: +1-510-642-7428.
E-mail address: getz@nature.berkeley.edu.

0040-5809/03/$ - see front matter
doi:10.1016/S0040-5809(03)00026-1

are even more difficult to tease out in systems of interacting populations.

Correlations of variation among ecologically interacting populations, as well as correlations between populations and environmental variables (e.g. rainfall, temperature, nutrients), can be obtained from the residuals of detrended time series obtained for such assemblages. An assemblage of n time series yields $n(n-1)/2$ pair-wise correlations before time-delayed correlations are taken into account. The existence of a single measure that reflects the degree to which an assemblage of n time series (or signals) are mutually correlated would be very useful in defining the coherence of the assemblage as a unit or object in its own right. Such a measure could be referred to as the *correlative coherence* of the assemblage.

Currently no method has been proposed for measuring the correlative coherence of an assemblage of n signals. Simply taking the average of the $n(n-1)/2$ pair-wise correlations r_{ij}, $i>j$, $i,j=1,\ldots,n$, is inconsistent because such assemblages represent at most n independent processes implying that the $n(n-1)/2$ correlations are not independent of one another. Bases invariant properties of all diagonalizable matrices are uniquely characterized by their eigenvalues and eigenvectors (see any linear algebra text, such as Noble and Daniel, 1977). Thus, I use the n eigenvalues of the correlation coefficient matrix $\mathbf{R}$ (i.e. matrix of $n(n-1)/2$ pair wise correlation coefficients $r_{ij}=r_{ji}$, $i>j$, $i,j=1,\ldots,n$, and $r_{ii}=1$, $i=1,\ldots,n$) to construct a generalized coherence measure for an assemblage of n signals. My measure is based on the Shannon–Weaver information measure (Shannon and Weaver, 1949) and I refer to its application in the context of investigating the coherence of sets and subsets of signals as *correlative coherence analysis* (CCA).

Applications of CCA go well beyond the population ecology example developed here. They include assessing the degree to which a sector of the stock market is driven by particular economic indices, whether a set of neurons responds to selected sensory stimuli, or how tightly a group of biological populations interact to form an ecological community. CCA complements rather than competes with existing multivariate methods, such as principle components (PCA—e.g. see Noble and Daniel, 1977) or factor analysis: CCA provides a holistic view of multivariable systems by using information contained across all the eigenvalues of the associated correlation matrix, while PCA and factor analysis focus only on information contained in the several most dominant eigenvalues and eigenvectors.

In this paper, I define a measure of correlative coherence and demonstrate that it ranges from 0 for uncorrelated systems to 1 for perfectly correlated or anticorrelated systems. I then illustrate how the measure can be used to explore the extent to which competing populations filter environmental stochasticity in trajectories generated by a nonlinear, discrete-time, two-species competition model. To provide a context for interpreting the results, I first look at how correlations between the trajectories of isolated populations, driven by a stochastic resource, are influenced by the level of stochasticity in the resource and the abruptness of density dependence in the model. I then analyze the coherence of two and three species, respectively, competing for two and three independently varying resources.

2. Methods

2.1. Correlative coherence analysis

For any pair of signals (X,Z) representing a sequence of scalar values—such as a detrended population trajectory $X=\{x(0),x(1),x(2),x(3),\ldots\}$ and an environmental time series $Z=\{z(0),z(1),z(2),z(3),\ldots\}$—define

$$\mathrm{Cor}_{XZ}(\delta)=\frac{\sum_{t=\delta}^{T}(x(t)-\bar{x})(z(t-\delta)-\bar{z})}{\sqrt{\sum_{t=\delta}^{T}(x(t)-\bar{x})^2\sum_{t=0}^{T-\delta}(z(t)-\bar{z})^2}}, \tag{1}$$

where $\bar{x}=(1/(T-\delta))\sum_{t=\delta}^{T}x(t)$ and $\bar{z}=(1/(T-\delta))\sum_{t=0}^{T-\delta}z(t)$. Thus, $-1\leqslant\mathrm{Cor}_{XZ}(\delta)\leqslant 1$ is the usual cross-correlation coefficient for signals X and Z over the time interval $[0,T]$, where the signal X has been right shifted by δ units (for a left shift just swap the roles of the X and Z). The value 1 arises when the two signals vary in an identical manner. Also $\mathrm{Cor}_{XZ}(\delta)\to 0$ as $T\to\infty$ for all values of δ whenever X and Z vary independently of one another. Further, two signals are regarded as perfectly coherent or entrained with one another if $\mathrm{Cor}_{XZ}(\delta)=-1$ because $\mathrm{Cor}_{XZ}(\delta)=-1\Rightarrow\mathrm{Cor}_{(-X)Z}(\delta)=\mathrm{Cor}_{X(-Z)}(\delta)=1$.

For any set of n signals $\mathbf{X}^n=\{X_1,\ldots,X_n\}$, where $X_i=\{x_i(0),x_i(1),x_i(2),\ldots\}$, the n^2 values $\mathrm{Cor}_{X_iX_j}(\delta_{ij})$, $i,j=1,\ldots,n$, selected so that $|\mathrm{Cor}_{X_iX_j}(\delta_{ij})|$ is maximized over all possible values of δ_{ij}, can be arranged as a symmetric matrix $\mathbf{R}$ with elements $r_{ij}=\max|\mathrm{Cor}_{X_iX_j}(\delta_{ij})|=r_{ji}$ (from Eq. (1) it follows that $\mathrm{Cor}^{\delta_{ij}}_{X_iX_j}(\delta_{ij})=\mathrm{Cor}_{X_jX_i}(\delta_{ij})$ with $\delta_{ij}=-\delta_{ji}$) and $r_{ii}=1$ (Eq. (1) implies $\mathrm{Cor}_{X_iX_i}(0)=1$).

The matrix $\mathbf{R}$ is thus a correlation matrix and its eigenvalues λ_i, $i=1,\ldots,n$, are known to satisfy $0\leqslant\lambda_i\leqslant n$ and $\sum_{i=1}^{n}\lambda_i=n$ (e.g. see Davies and Higham, 2000), which implies $0\leqslant\lambda_i/n\leqslant 1$ and $\sum_{i=1}^{n}\lambda_i/N=1$. Thus

$$C(\mathbf{X}^n)=1-\frac{1}{\ln(1/n)}\sum_{i=1}^{n}\left(\frac{\lambda_i}{n}\right)\ln\left(\frac{\lambda_i}{n}\right) \tag{2}$$

is a well-defined Shannon–Weaver-type measure (Shannon and Weaver, 1949) of the diversity of eigenvalues λ_i.

Further, if all signals in $\mathbf{X}^n$ are completely uncorrelated, the matrix $\mathbf{R}$ approaches (as the length of the signals increase) the identity matrix for which $\lambda_i = 1,\ i = 1, \ldots, n$. From expression (2) this implies $C(\mathbf{X}^n) = 0$. Also, if all the signals are perfectly correlated, then all the elements of $\mathbf{R}$ are 1. In this case, the eigenvalues satisfy (Morrison, 1976, Section 8.5) $\lambda_1 = n,\ \lambda_2 = \lambda_3 = \cdots = \lambda_n = 0$, which, from expression (1) implies $C(\mathbf{X}^n) = 1$.

Expression (2) can be regarded as generalizing the well-known concept of coherence for periodic signals and provides a measure of the degree to which the signals $\mathbf{X}^n$ vary in concert with, or are independent of, one another (Bendat and Piersol, 1966). Further, linear and nonlinear trends may be removed by using the residuals of the signals, after being fitted by some appropriate model, rather than the signal itself. Note that for any set of signals $\{X_1, \ldots, X_n\}$, $C(\mathbf{X}^n)$ is invariant with respect to the sign of the correlations r_{ij} because the correlation matrices associated with all permutations of $\{\pm X_1, \ldots, \pm X_n\}$ with regard to sign have the same eigenvalues. This is easily verified using diagonal matrices with 1's and -1's on the diagonal to perform similarity transformations among the correlation matrices.

If all off-diagonal correlations have the same value $r \in [0, 1]$ (the diagonal elements remain 1), the eigenvalues of the correlation matrix $\mathbf{R}(r)$ are known to be $\lambda_1 = 1 + (n-1)r$ and $\lambda_i = 1 - r$ for $i = 2, \ldots, n$ (Morrison, 1976, Section 8.5). In this case, expression (2) reduces to

$$C_n(r) = \frac{(1 + (n-1)r)\ln(1 + (n-1)r) + (n-1)(1-r)\ln(1-r)}{n \ln n}. \tag{3}$$

Thus, as required, if $r = 0$ then $C(\mathbf{X}^n) = 0$ (completely uncorrelated case with $\lambda_i = 1,\ i = 1, \ldots, n$), and if $r = 1$ then $C(\mathbf{X}^n) = 1$ (perfectly correlated case with $\lambda_1 = n,\ \lambda_i = 0,\ i = 2, \ldots, n$).

For $0 < r < 1$ expression (3) implies that $C_m(r) > C_n(r)$ whenever $m > n > 1$ (Fig. 1). Thus, measure (3) increase with the dimension of the signal assemblage, but the coherence of any two systems $\mathbf{X}^n$ and $\mathbf{Y}^m$, can always be compared through the values of r that solve $C_n(r) = C(\mathbf{X}^n)$ and $C_m(r) = C(\mathbf{Y}^m)$ (Fig. 1). Since C_n^{-1}, the inverse function of $C_n(r)$ defined by Eq. (3), exists because $C_n(r)$ is monotonic (Fig. 1), the correlative coherence r of any system $\mathbf{X}^n$ is the solution to the equation

$$r = C_n^{-1}(C(\mathbf{X}^n)). \tag{4}$$

Comparisons of two values $r_1 = C_n^{-1}(C(\mathbf{X}^n))$ and $r_2 = C_n^{-1}(C(\mathbf{X}^m))$, where $\mathbf{X}^m \subset \mathbf{X}^n$, can also be used to address the questions of how correlative coherence changes by the addition or subtraction of one or more signals from some set, and whether the correlative coherence is significantly increased by the addition of a specific signal relative to the affect of a signal not correlated with any of the others in the set.

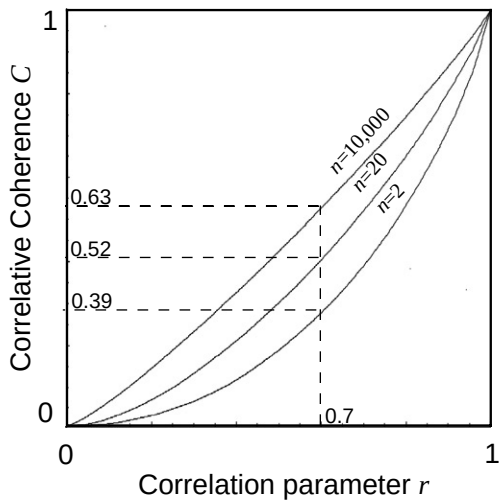

Fig. 1. The correlative coherence value $C_n(r)$ (see Eq. (3)) is plotted as a function of the correlation parameter r for the cases $n = 2$, 20, and 10,000. The dotted lines indicate how values of $C(\mathbf{X}^2) = 0.39$, $C(\mathbf{X}^{20}) = 0.52$, and $C(\mathbf{X}^{10,000}) = 0.63$ all yield the same solution $r = 0.7$ to Eq. (4).

In empirical studies, hypotheses regarding the significance of differences in the correlative coherence values of two sets of signals can be tested using bootstrap or jackknife methods (e.g. see Section 5.6 in Venables and Ripley, 1997) to estimate standard errors associated with the various correlative coherence values. These estimates are made in the usual way by omitting different subsets of points indexed by t in calculation of correlations using Eq. (1). Specifically, for a given set of signals and given subsets of indeces $T_j,\ j = 1, \ldots, m$, resulting in corresponding omissions of terms in the sum defined in Eq. (1) (jackknifing corresponds to the case $m = T$, and T_j represents omission of the jth term in Eq. (1)) calculation of the jth correlative coherence estimate r_j is made using Eqs. (2)–(4). Variation in these estimates is then used in the usual way to generate standard error estimates (Venables and Ripley, 1997) for the correlative coherence of the sets of signals to be compared.

2.2. Population model

In this section, I present details of a model used to demonstrate CCA analysis in the context of a theoretical study of populations competing for a set of independent stochastic resources. The dynamics underlying the populations in this analysis is the single-population model (Getz, 2001)

$$x(t+1) = g(\phi(x(t), z(t)))x(t), \tag{5}$$

where $x(t) \geqslant 0$ is the density of a population at time t growing on a resource at density $z(t) \geqslant 0$. The function

$\phi(x,z)$ represents the amount of resources that each individual is able to ingest (i.e. extract from its environment) during its life and $g(\phi)$ is the reproductive value of each individual at birth.

Assume the per-capita resource extraction process $\phi(x,z)$, regulated through intraspecific competition, is expressed in terms of the Beddington function (Beddington, 1975; DeAngelis et al., 1975; Getz, 1984, 1991, 1993, 1994)

$$\phi(x,z)=\frac{az}{b+cx+z}, \tag{6}$$

where $a>0$, $b>0$, and $c>0$, respectively, are the maximum resource extraction rate, the extraction efficiency, and the interference competition parameters. Further, assume that the reproductive value (or growth function) g has the generalized Beverton and Holt form (Getz, 2001)

$$g(\phi)=\frac{\rho\phi^{\gamma}}{k^{\gamma}+\phi^{\gamma}}, \tag{7}$$

where $\rho>1$ is the maximum growth rate realized when resources are not limiting, $k>0$ is the resource intake level at which the growth rate of the population is half the maximum rate, and $\gamma>1$ the abruptness of the density dependence (Getz, 1996). In this case Eqs. (5)–(7) can be combined to yield the discrete time dynamic model

$$x(t+1)=\frac{\rho(az(t))^{\gamma}}{(kb+kcx(t)+kz(t))^{\gamma}+(az(t))^{\gamma}}x(t). \tag{8}$$

For constant z, this model is very similar to a model that has been extensively analyzed in terms of the influence of the parameter γ on the stability and chaotic structure of solutions and analytical expressions for the nontrivial equilibrium solution and the values of γ at which solutions bifurcate to oscillatory and chaotic are easily derived (Getz, 1996; Schoombie and Getz, 1998). When the resource $z(t)$ has the stochastic form

$$z(t)=z_0+z_1v(t), \tag{9}$$

where $0\leqslant z_1\leqslant z_0$ are constants and $v(t)$, $t=0,1,2,\ldots$ is a sequence of independent, identically distributed, uniform random variables on the interval $[-1,1]$, then solutions to Eq. (8) can be generated numerically, using an appropriate random number generator.

Here we are more interested in simulating solutions when the model has been generalized to m competitors at densities $\mathbf{x}(t)=(x_1(t),\ldots,x_m(t))'$ exploiting m resources at densities $\mathbf{z}(t)=(z_1(t),\ldots,z_m(t))'$ (the symbol $'$ denotes vector transpose). In this case the extraction functions in the m-population model

$$x_i(t+1)=g_i(\phi_i(\mathbf{x}(t),\mathbf{z}(t))x_i(t),\quad i=1,\ldots m \tag{10}$$

generalize to

$$\phi_i(\mathbf{x},\mathbf{z})=\frac{a_i\sum_{j=1}^{m}p_{ij}z_j}{b_i+c_i\sum_{j=1}^{m}p_{ij}x_j+\sum_{j=1}^{m}p_{ij}z_j},$$
$$i\bullet j,\quad i,j=1,\ldots m, \tag{11}$$

where $0\leqslant p_{ij}\leqslant 1$ represents the degree of niche overlap for the two species (Getz, 2001) and, from Eq. (7), $g_i(\phi_i)=\rho_i\phi_i^{\gamma_i}/(k_i^{\gamma_i}+\phi_i^{\gamma_i})$. Symmetry and normalization considerations imply $p_{ii}=1$ and $p_{ij}=p_{ji}$, $i,j=1,\ldots,m$. If p_{ij} are much closer to 0 than 1 for all $i\bullet j$, $i,j=1,\ldots,m$, then competition is insignificant and population i can be regarded as a specialist on resource i, for $i=1,\ldots,m$. Also, if the values p_{ij} are close to 1 for some $i\bullet j$, then competition between population i and j is intense and one of them may be competitively excluded by the other, depending on the relative values of the various population parameters and how these populations are affected by having to compete with the remaining populations. For interacting species, the resource equations generalize to

$$z_i(t)=z_{i0}+z_{i1}v_i(t),\quad i=1,\ldots,m, \tag{12}$$

where $z_{i0}\geqslant z_{i1}\geqslant 0$ and $v_i(t)$ and $t=0,1,2,3\ldots$ are sequences for $i=1,2,3$, of independent uniformly distributed random variables on $[-1,1]$. More generally, we could allow for variation in the resources to be correlated, but this would unnecessarily complicate the analysis without adding any fundamental insights.

The baseline parameter values for deterministic, single-population simulations presented here are $a=10$, $b=10$, $c=1$, $\rho=5$, and $k=1$; and for the noise they are $z_0=10$ (Table 1, Fig. 2). The baseline parameters for the two $(i=1,2)$ and three $(i=1,2,3)$ competing species models are $a_1=15$, $a_2=10$, $a_3=12.5$, $b_1=b_2=b_3=10$, $c_1=c_2=c_3=1$, $\rho_1=\rho_2=\rho_3=5$, $k_1=k_2=k_3=1$, $\gamma_1=7$, $\gamma_2=3$, and $\gamma_3=5$, and for the deterministic component of the noise they are $z_{10}=z_{20}=z_{30}=10$ (Figs. 2 and 3).

3. Results

3.1. Variation in a single population

The parameter γ in Eq. (7) can be used to increase the abruptness of the change of net-reproductive rate with population density from a gentle sigmoidal decline for γ close to 1 (the sigmoidal inflection disappears at $\gamma=1$ when the function becomes a hyperbola) to a virtual step-down function for γ much beyond 20 (Getz, 1996). Also, for any given set of parameters a,b,c,k,ρ, and z_0 in the deterministic version of Eqs. (8) and (9) (i.e. $z_1=0$), increasing the value of γ will cause the equilibrium solution to this equation to undergo a series

Table 1
The mean values $\bar{x}$ of trajectories[a] and values of associated coefficients of variation[a] CV_x and CV_z for the state and noise respectively, are tabulated for the density-dependent abruptness parameter γ ranging from 1 to 10 and the degree-of-stochasticity parameter z_1 ranging from 0 to 10. The baseline parameters used to obtain these results from Eqs. (8) and (9) are $a = 10$, $b = 10$, $c = 1$, $\rho = 5$, $k = 1$, $z_0 = 10$

γ	Dynamic properties	$z_1 = 0$ $CV_z = 0$	1 0.06	2 0.12	5 0.29	8 0.46	9 0.52	10 0.58
1	Stable equilibrium	$x = 380$ $CV_x = 0$	380 0.05	378 0.09	367 0.24	342 0.41	327 0.48	300 0.60
2	Stable equilibrium	$x = 180$ $CV_x = 0$	180 0.10	178 0.19	175 0.41	160 0.63	151 0.73	131 0.90
3	Stable 2-cycle {91,192}	$\bar{x} = 142$ $CV_x = 0.36$	141 0.33	140 0.38	133 0.59	116 0.85	106 0.97	88 1.20
4	Stable 4-cycle {161,68,212,35}	$\bar{x} = 119$ $CV = 0.59$	119 0.56	118 0.58	109 0.78	93 1.06	84 1.20	66 1.49
5	Stable 3-cycle[b] {12,62,266}	$\bar{x} = 100$ $CV_x = 0.91$	102 0.73	101 0.76	92 0.96	78 1.26	74 1.41	52 1.77
7	Chaos	$\bar{x} = 76$ $CV_x = 1.08$	77 1.05	76 1.08	70 1.27	58 1.60	51 1.78	35 2.30
10	Chaos	$\bar{x} = 56$ $CV_x = 1.38$	55 1.44	55 1.46	50 1.66	42 2.04	37 2.25	22 3.09

[a] The first values in rows 1 and 2 are actually equilibria. The remaining are mean values estimated here along with the CVs to ± 0.01 using 500,000 iterations per run (in some cases averaged over 3 to 4 repeated runs).
[b] Beyond point of period doubling bifurcations which approach chaos at around $\gamma = 4.10$.

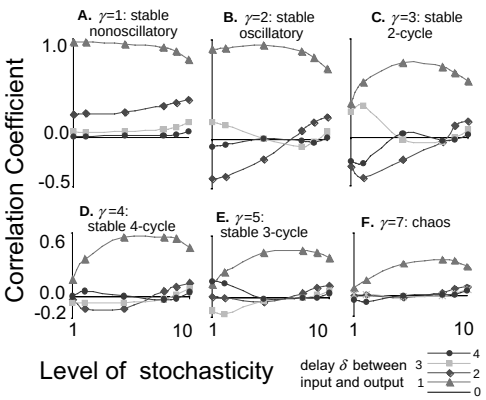

Fig. 2. The correlation coefficients $Cor_{xz}(\delta)$, $\delta = 0$ to 4 are plotted as functions of the noise parameter z_1 (over the interval 1 to 10—see Table 2) for the 6 cases A–F, respectively, involving increasing levels of abruptness in the density dependence as given by the parameter values $\gamma = 1, 2, 3, 4, 5$ and 7, where the other parameters in the model are the baseline values (Table 1). The attractors associated with the dynamics of the 6 cases are: (A) a stable node, (B) a stable center, (C) a stable 2-cycle, (D) a stable 4 cycle, (E) a stable 3 cycle that occurs beyond the point of bifurcation to chaos at $\gamma = 4.1$, and (F) a strange attractor.

of period-doubling flip bifurcations (see Feigenbaum, 1980) from being stable with regard to the baseline set of parameters (Table 1) for $\gamma < 2.85$ (rounding to 2 decimal places) to entering the chaotic regime at approximately $\gamma = 4.10$. Properties of the trajectories (stable equilibrium values or mean values, stable cycles when present, coefficients of variation when variable) for parameter values $\gamma = 1$, 2, 3, 4, 5,7 and 10 are given in Table 1.

Under deterministic conditions ($z_1 = 0$ column in Table 1), due to the effect of increasing abruptness in density dependence, the mean value of the trajectory over 500,000 iterations (or equilibrium value for small γ) declines from 380 when $\gamma = 1$–56 at $\gamma = 10$ (Table 1). For given levels of abruptness in the density dependence (i.e. values of γ), high levels of noise (due to environmental stochasticity) also cause marked declines in mean population densities. This is particularly true under chaotic conditions where a 2–3 fold decline in mean population density is observed (cf. 56 at $z_1 = 0$ versus 22 at $z_1 = 10$ in the bottom row of Table 1). In the most stable case ($\gamma = 1$), the highest noise ($z_1 = 10$) produces only moderate levels of variability in the output (the coefficient of variation is $CV = 0.6$—Table 1). With increasing levels of abruptness in the density dependence, not only does the coefficient of variation increase to levels beyond $CV = 1$ for the deterministic cases (cf. last two rows of $z_1 = 0$ column in Table 1), but the noise is magnified so that at the highest noise levels the total CV for the most abrupt density-dependent case exceeds 3 (viz., when $\gamma = 10$ and $z_1 = 10$, $CV = 3.09$—Table 1). This result implies that the nonlinearity associated with density dependence has the effect of amplifying

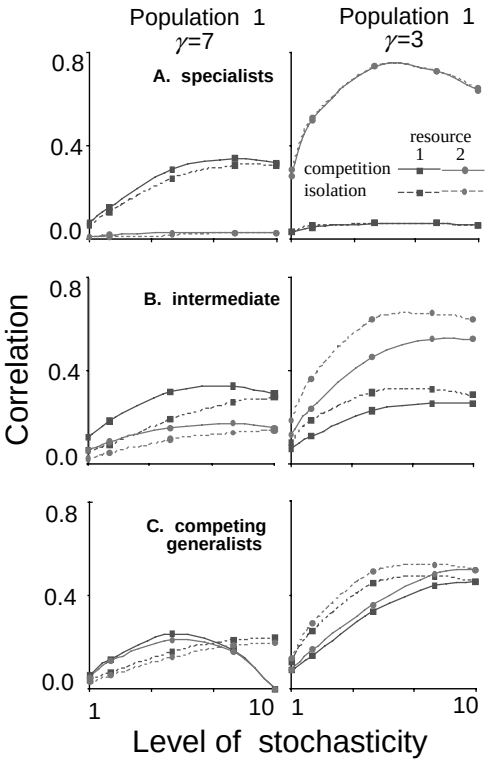

Fig. 3. The correlation coefficients $\mathrm{Cor}\,C(x_i z_j)$ (competition: solid lines in all panels) and $\mathrm{Cor}\,I(x_i z_j)$ (isolation: dotted lines in all panels) are plotted for population 1 ($i=1$, left panels A–C) and population 2 ($i=1$, right panels A–C) and for resources 1 ($j=1$, lines with square markers) and resources 2 (lines with round markers) as functions of the noise parameter z_1 over the interval 1 to 10 for the three levels of competition: (A) $p=0.1$, (B) $p=0.5$, and (C) $p=0.9$.

variation in the noise only when this variation is relatively large (i.e. for noise CVs approaching 0.5). For example, if we use the notation $\mathrm{CV}_x(\gamma, z_1)$ and $\mathrm{CV}_z(z_1)$ to, respectively, denote the CVs of the system trajectory and the noise for specific values γ and z_1, then from Table 1 it is apparent that for large noise

$$\mathrm{CV}_x(10,0)+\mathrm{CV}_z(10)=1.38+0.58 = 1.96 \ll \mathrm{CV}_x(10,10)=3.09,$$

while for small noise

$$\mathrm{CV}_x(10,0)+\mathrm{CV}_z(2)=1.38+0.12 = 1.50 > \mathrm{CV}_x(10,2)=1.46.$$

For all values of γ, the correlation between the population and the noisy resource is zero when the delay is zero (i.e. $\delta=0$—see Figs. 2A–F). This, of course, is expected because in the model the value of the resource z at time t does not influence the value of the state x at time t, but only at time $t+1$ (cf. Eq. (8)). Further, irrespective of the level of abruptness represented the density-dependence parameter γ or the level of the noise z_1 the correlations are larger for $\delta=1$ than any other value of δ. As δ increases beyond 1, the patterns of correlation values, as elaborated below, depend on whether the solution is stable, oscillatory, or chaotic and whether the noise is low, moderate, or high.

At $\gamma=1$, the system is most stable (as shown in Getz (1996) systems of this type are stable for $\gamma=1$ no matter how large the value of the parameter ρ, while for $\gamma=2$ the system becomes unstable if ρ is sufficiently large). The correlation between the population and the noise drops for $\mathrm{Cor}_{XZ}(1)=0.97$ (see Eq. (1)) to $\mathrm{Cor}_{XZ}(1)=0.79$ as the level of noise increases from $z_1=0$–10 (Fig. 2A). At $\gamma=2$, the system is still stable for the baseline set of parameters, but now the highest correlation between the population and the resource is not achieved at the lowest noise levels, but at intermediate noise levels ($\mathrm{Cor}_{XZ}(1)=0.90$ at $z_1=1$, $\mathrm{Cor}_{XZ}(1)=0.95$ at $z_1=5$, and $\mathrm{Cor}_{XZ}(1)=0.71$ at $z_1=10$—Fig. 1B). Also, for low-to-moderate noise levels ($z_1=1$–5) the trajectories are negatively correlated with noise two time periods back and positively correlated with noise three time periods back because the approach of the trajectory to the equilibrium is oscillatory (e.g. when $\gamma=2$, $\mathrm{Cor}_{XZ}(2)$ rises from -0.39 to -0.20 and $\mathrm{Cor}_{XZ}(3)$ drops from 0.14 to 0.01 as z_1 increases from 1 to 5—Fig. 2B). The same phenomenon is observed more strongly for the case $\gamma=3$ when the equilibrium is unstable, but the two cycle {91,192} is stable (Fig. 2C). In this case, the correlation is still relatively strong between the trajectory and the noise and alternating in sign for four, five, six and more periods back (e.g. for $z_1=2$, $\mathrm{Cor}_{XZ}(4)=-0.26$—see Fig. 2C; also not shown $\mathrm{Cor}_{XZ}(5)=0.22$ and $\mathrm{Cor}_{XZ}(6)=-0.18$).

A nonobvious effect is that the correlations between the trajectory and the noise one time-step back peak at increasingly higher noise levels as the levels of abruptness in the density dependence increases (Figs. 2A–E). For example, $\mathrm{Cor}_{XZ}(1)$ peaks around $z_1=1$ when $\gamma=1$ (Fig. 2A), around $z_1=6$ when $\gamma=3$ (Fig. 2C), and around $z_1=8$–9 when $\gamma=7$ (Fig. 2E). Additionally, for relatively abrupt density dependence (cf. Fig. 2F and for $\gamma>9$—not shown) all correlations are severely degraded beyond the first time delay. Again, not obvious, is the fact that correlations disappearing at moderate noise levels reappear as small positive correlations at the noisiest levels (e.g. when $\gamma=5$, $\mathrm{Cor}_{XZ}(4)=0.00$ for $z_1=8$ and 9, but $\mathrm{Cor}_{XZ}(4)=0.04$ when $z_1=10$—Fig. 2E; when $\gamma=7$, $\mathrm{Cor}_{XZ}(4)=0.00$ when $z_1=5$, but $\mathrm{Cor}_{XZ}(4)=0.04$ when $z_1=10$—Fig. 2F; and, not illustrated, when $\gamma=10$, $\mathrm{Cor}_{XZ}(2)=0.00$ when $z_1=1$, but $\mathrm{Cor}_{XZ}(2)=0.06$ when $z_1=10$).

3.2. Variation in two competing populations

The competing species model can be simulated using initial conditions in which either one of the populations is zero or both are nonzero. If a population is initially 0,

it remains 0 throughout the simulation. Thus, when its competitor is 0, I will refer to the correlation between a population and either of the stochastic resources as the isolated correlations and denote such correlations by Cor $I(x_i z_j)$ (the time-delay in this case is taken to be $\delta = 1$ because of the natural dependence of population density on resource density at the previous time step). When both populations are present, and hence competing, I denote this same correlation calculation (i.e. Eq. (1)) by Cor $C(x_i z_j)$ and the additional correlation of the two populations by $\mathrm{Cor}(x_1 x_2) \equiv \mathrm{Cor}_{x_1 x_2}(0)$. (Note, in this case, $\delta = 0$ because neither population is privileged with regard to timing in its influence on the other population—cf. Eq. (1).)

To keep the analysis simple, the results reported here were obtained under the assumption that both resources exhibited the same level of variation z_1 (i.e. $z_{11} = z_{21} \coloneqq z_1$—cf. Eqs. (12)). In this case, when the niche or competition parameter $p = p_{12} = p_{21}$ (cf. Eqs. (11)) is small, so that each species exploits mainly its own special resource, then the correlation coefficients for both species in isolation from one another are very similar to the corresponding correlation coefficients for the two species coexisting—in fact, for $p = 0.1$, the values are still almost identical (Fig. 3A). As expected from the results obtained for a single population (Fig. 1), the correlations obtained from the two-population model for competing specialists (Figs. 3A), are stronger for species 2 than 1 because of the higher level of abruptness in the density dependence in species 2 ($\gamma_2 = 7$) than 1 ($\gamma_1 = 3$). Also, each species is more strongly correlated to the resource on which it specializes (i.e. Cor $C(x_1 z_1) \gg$ Cor $C(x_1 z_2)$ and Cor $C(x_2 z_2) \gg$ Cor $C(x_2 z_1)$—see Fig. 3A), because each fully exploits its preferred resource while only exploiting 10% ($p = 0.1$) of its less-preferred resource.

At the other extreme, when the niche parameter p is close to 1, the species compete head on for both resources so that their correlations with either resource are similar (i.e. Cor $C(x_1 z_1) \approx$ Cor $C(x_1 z_2)$—see Fig. 3C). In this case, however, the correlations for the populations in isolation from one another are very different from the corresponding correlations under coexistence because the effects of competition on these correlations are strong. In particular, at low-to-moderate noise levels ($z_1 = 1$–6) competition causes the following effects: (i) intrinsically chaotic population 1 ($\gamma_2 = 7$: see Table 1) entrains more of the noise (i.e. Cor $C(x_1 z_j) >$ Cor $I(x_1 z_j)$, $j = 1, 2$—see Fig. 3C left panel) and hence behaves like a population that has a lower level of abruptness in the density dependence (i.e. a smaller value of γ than 7), (ii) population 2, which has a stable 2 cycle ($\gamma_2 = 3$: see Table 1), entrains less of the noise (i.e. Cor $C(x_2 z_j) <$ Cor $I(x_2 z_j)$, $j = 1, 2$—see Fig. 3C right panel) and hence behaves like a population that has a higher level of abruptness in the density dependence (i.e. a larger value of γ than 3). In short, at low to intermediate noise levels, competition causes each of two populations to become more alike in the way they entrain noise than they do in isolation from one another.

At high noise levels, this "averaging" of the density-dependent effects breaks down. The reason is that at high noise levels, population 1 the inferior competitor is ultimately excluded by population 2 at the highest noise level ($z_1 = 10$), which is why at this noise level Cor $C(x_1 z_1) =$ Cor $C(x_1 z_2) = 0$ (Fig. 3C left panel). At intermediate levels of specialization and, hence, competition, the results are intermediate (Fig. 3B) between the two extremes (Figs. 3A and C). Also, at this intermediate level of competition, population 2 is unable to exclude population 1, as occurs under intense competition.

The results presented in Figs. 2 and 3 rely upon comparisons of correlation coefficients under different sets of circumstances (differences in noise levels, levels of abruptness in the density dependence, and intensity and contexts of competition) and provide a basis for comparisons with the correlative coherence of higher dimensional sets of signals—in particular, for the system $\{X_1, X_2, Z_1, Z_2\}$. The correlative coherence r of this system (see Eq. (4)), denoted for convenience by $\mathrm{Cor}(x_1 x_2 z_1 z_2) \equiv r$, permits us to compare the correlative coherence of the system to any subset of the system, including the individual correlation coefficients of any two variables in the system. In particular, compare the values $\mathrm{Cor}(x_1 x_2)$, and $\mathrm{Cor}(x_1 x_2 z_1 z_2)$ as functions of the noise level z_1 (recall $z_1 = z_{11} = z_{21}$) for the three competition levels $p = 0.1$, 0.5 and 0.9 (Fig. 4).

At low noise levels, the correlation $\mathrm{Cor}(x_1 x_2)$ between the populations is equal to the correlative coherence $\mathrm{Cor}(x_1 x_2 z_1 z_2)$ of the whole system at low competition levels (Fig. 4A). The correlation $\mathrm{Cor}(x_1 x_2)$, however, rises more rapidly than the correlative coherence $\mathrm{Cor}(x_1 x_2 z_1 z_2)$ (Figs. 4B and C). As noise levels increase, however, the correlative coherence $\mathrm{Cor}(x_1 x_2 z_1 z_2)$ exceeds the correlation $\mathrm{Cor}(x_1 x_2)$ at low competition levels for moderate noise (Fig. 4B) but exceeds it at all competition levels when the noise is high (Fig. 4C). The reason is that with increasing noise, correlations

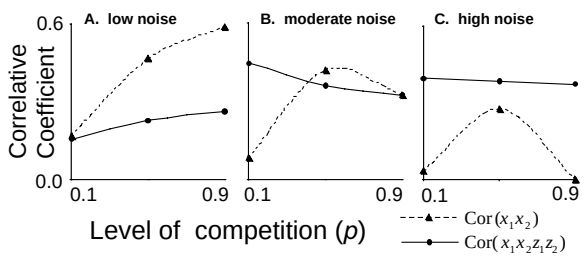

Fig. 4. The correlation $\mathrm{Cor}(x_1 x_2)$, (broken lines) and the correlative coherence coefficients $\mathrm{Cor}(x_1 x_2 z_1 z_2)$ (solid lines) are plotted as functions of the competition parameter p ranging from 0.1 to 0.9 for the three noise levels: (A) $z_1 = 1$, (B) $z_1 = 5$, and (C) $z_1 = 10$.

between the populations and the environmental variables strengthen to the point where they dominate correlations that arise from competitive interactions. Again, note that correlations between the populations fall to zero at the highest noise levels when competition is strongest (Fig. 4C) because one of the populations is excluded by the other.

3.3. Variation in three competing populations

Simulations of Eqs. (10)–(12) for the case, $n=3$, yields fifteen different correlations: for $i,j=1,2,3$, $\mathrm{Cor}(x_i z_j)$ (recall $\delta=1$ for these 9 correlations); additionally for $i<j$, $\mathrm{Cor}(x_i x_j)$ (recall $\delta=0$ for these 3 correlations) and $\mathrm{Cor}(z_i z_j)$ (these 3 correlations are 0 because the resources vary independently). We already have a sense from Figs. 2–4 of how these 15 correlations depend on the level of competition among populations, the level of variation in the resources, and the level of abruptness in the density-dependent resource extraction function. Thus we now focus on the correlative coherence values of the three two-population subsystems $\{X_i, X_j, Z_i, Z_j\}$, $j>i$, $i,j=1,2,3$, compared with the correlative coherence of the total system $\{X_1, X_2, X_3, Z_1, Z_2, Z_3\}$ in terms of levels of competition and noise, and levels of abruptness in the density dependence. Note our analysis here of the various subsystems uses the trajectories generated by the model when all populations are present, rather than the isolated subsystems that would arise if we removed each of the three populations in turn by setting its initial value to zero.

Over the range of parameter values used in the simulations (Fig. 5), the smallest total coherence value $\mathrm{Cor}(x_1x_2x_3z_1z_2z_3)$ occurs at the lowest competition, lowest noise level (Fig. 5A) while the largest total coherence value $\mathrm{Cor}(x_1x_2x_3z_1z_2z_3)$ occurs also at the lowest noise level, but this time for intermediate to high competition levels (Fig. 5A). The subsystem that is most coherent, except when competition and noise are both at intermediate to high levels, is $\{X_2, X_3, Z_2, Z_3\}$ (Figs. 5A and C). Note this subsystem includes the populations with the two lowest levels of abruptness in the density dependence of the exploitation functions ($\gamma_3=3$, and $\gamma_2=5$). The subsystem that is least coherent depends on the particular combination of competition and noise. Except at low competition levels, the subsystem $\{X_1, X_2, Z_1, Z_2\}$, which includes the populations with the two highest levels of abruptness in the density dependence of the exploitation functions ($\gamma_1=7$, and $\gamma_2=5$), has the lowest correlative coherence at low and intermediate noise levels. Interestingly, the subsystem $\{X_1, X_3, Z_1, Z_3\}$, which includes the highest and lowest levels of abruptness in the density dependence of the exploitation functions ($\gamma_1=7$, and $\gamma_3=3$) is the least coherent of the three subsystems at the lowest level of competition ($p=0.1$) for low-(Fig. 5A)-to-moderate (Fig. 5B) noise levels and for highest competition levels ($p=0.9$) at the highest noise levels (Fig. 5C).

The correlative coherence of the total system $\{X_1, X_2, X_3, Z_1, Z_2, Z_3\}$ is, in all cases, intermediate between the lowest and highest levels of correlative coherence of the component systems. At the lowest noise level, however, the total system values are closer to the maximum than minimum sublevel over most of the range of competition values (Fig. 5A), while at the highest noise level the total system values are close to the minimum of over most of the range of competition values (Fig. 5C). If we focus on the correlative coherence of the system time series $\{X_1, X_2, X_3\}$ alone, then again we find that $\mathrm{Cor}(x_1x_2x_3)$ is intermediate between the highest and lowest values of $\mathrm{Cor}(x_ix_j)$, $i>j, i,j=1,2,3$, over the range of noise levels z_1 for all competition parameters p (Figs. 6A–C). If we compare the correlative coherence of the entire system to any subsystems that ignore the environmental variables, however, the picture is substantially altered. At low competition levels, the population-only correlative coherence $\mathrm{Cor}(x_1x_2x_3)$ is several-fold less than the complete system correlative coherence $\mathrm{Cor}(x_1x_2x_3z_1z_2z_3)$, except at the lowest noise levels where this relationship is

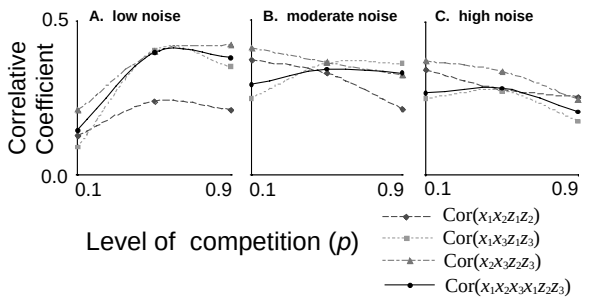

Fig. 5. The correlative coherence coefficients for the three subsystems $\{X_i, X_j, Z_i, Z_j\}$, $j>i$, $i,j=1,2,3$, (broken lines) and the total system $\{X_1, X_2, X_3, Z_1, Z_2, Z_3\}$ (solid line) are plotted as functions of the competition parameter p ranging from 0.1 to 0.9 for the three noise levels: (A) $z_1=1$, (B) $z_1=5$, and (C) $z_1=10$.

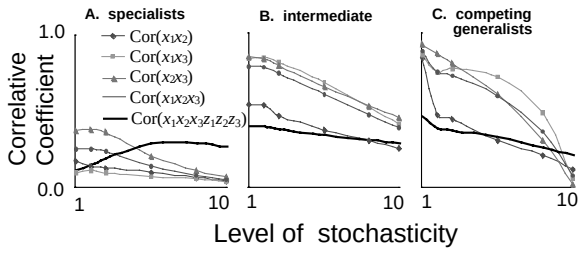

Fig. 6. The correlative coherence coefficients for three populations considered two at time, all three together, and for the total system $\{X_1, X_2, X_3, Z_1, Z_2, Z_3\}$ (thick solid line) are plotted as functions of the noise parameter z_1 over the interval 1 to 10 for the three levels of competition: (A) $p=0.1$, (B) $p=0.5$, and (C) $p=0.9$.

Table 2
The correlation coefficients are tabulated for two high noise ($z_1 = 10$) cases: (A) low competition ($p = 0.1$, cf. Fig. 6A), (B) high competition ($p = 0.9$, cf. Fig. 6C)

	X_2	X_3	Z_1	Z_2	Z_3
(A)					
X_1	0.04	0.03	0.34	0.03	0.03
X_2		0.07	0.06	0.67	0.06
X_3			0.04	0.04	0.45
Z_1				0.00	0.00
Z_2					0.00
(B)					
X_1	0.11	0.06	0.12	0.11	0.11
X_2		0.02	0.37	0.41	0.37
X_3			0.01	0.01	0.02
Z_1				0.00	0.00
Z_2					0.00

reversed (Fig. 6A). By contrast, at high competition levels, $\mathrm{Cor}(x_1x_2x_3)$ is substantially larger than $\mathrm{Cor}(x_1x_2x_3z_1z_2z_3)$, except at the highest noise levels where this relationship is reversed (Fig. 6C). At intermediate competition levels, $\mathrm{Cor}(x_1x_2x_3)$ is larger than $\mathrm{Cor}(x_1x_2x_3z_1z_2z_3)$ for all three noise levels. The reason why $\mathrm{Cor}(x_1x_2x_3z_1z_2z_3) \gg \mathrm{Cor}(x_1x_2x_3)$ for the low competition, high noise case ($p = 0.1$, $z_1 = 10$—see Fig. 6A) is that each population is strongly correlated with the variability in the primary resource that it exploits (Table 2A). The reason why $\mathrm{Cor}(x_1x_2x_3z_1z_2z_3) > \mathrm{Cor}(x_1x_2x_3)$ for the highest noise level in the high competition case ($p = 0.9$, $z_1 = 10$—see Fig. 6C) is that the most competitive population, which in this case is population 2 (for this case, the mean population values are $\bar{x}_1 = 30.1$, $\bar{x}_2 = 350.9$, and $\bar{x}_3 = 0.1$), has strong correlations with all three resource variables (Table 2B).

4. Discussion

To provide a context for interpreting multi-population systems, the analysis of isolated populations indicates that stable systems strongly entrain the noise (the case $\delta = 1$), irrespective of the actual noise level, but for oscillatory systems, the strongest level of entrainment is at an intermediate noise level and the strength of entrainment drops as the period of oscillation increases to infinity (i.e. chaos). The strength of cross-correlations (the cases $\delta > 1$), depend on the periodicity of attractors. The results suggest the following with regard to a population whose dynamics are primarily determined by intraspecific competition driven by stochastic resource inputs.

If the population–resource correlations range over (see Fig. 2):

- [0.75,1.00], then the population attractor is stable;
- [0.6, 0.75], then the population attractor is a two cycle and the resource noise level is intermediate to high;
- [0.35, 0.6], then the population attractor is a two cycle and resource noise levels are low, or the population attractor is in the neighborhood of the bifurcation to chaos (just below in the period-doubling regime, or just above), and resource levels are moderate to high;
- [0.1, 0.35], then the population attractor is strongly chaotic ($\gamma \geqslant 7$) and the noise is moderate to high.
- [0.0, 0.1], then the population attractor is chaotic ($\gamma > 4$) and the noise is low.

(Note that the resolution of Fig. 1 makes it difficult to accurately read the above bounds. The numbers come from numerical results used to produce panels A–C in Fig. 6).

Perhaps the most counter-intuitive of these results, which could not have been obtained without the use of a model, is that relatively chaotic systems (i.e. those with a deterministic CV_x exceeding 1.0) are entrained quite strongly by moderate-to-high levels of noise (i.e. correlations are in the neighborhood of 0.2–0.35), but not by low levels of noise (i.e. $z_1 < 2$, or a noise CV_z of less than 0.1). Also not intuitive is the fact that highly abrupt density dependence ($\gamma = 10$) amplifies large noise but dampens low noise.

Interspecific competition (with intensity denoted by the value of parameter $p = p_{12} = p_{21}$ in a two-population analysis) has the effect of reducing the entrainment of environmental driving variables on the intrinsically more stable population (i.e. population 2 with $\gamma = 3$) and increasing it on the less stable populations (i.e. population 1 with $\gamma = 7$): not unexpectedly, competition has the effect of regressing the degree to which each of the two populations entrain environmental variability on its own towards the mean of the two. For example, when $p = 0.9$ and $z_1 = 5$, $\mathrm{Cor}\, I(x_1z_1) = 0.16$ increases to $\mathrm{Cor}\, C(x_1z_1) = 0.24$ and $\mathrm{Cor}\, I(x_2z_1) = 0.45$ decreases to $\mathrm{Cor}\, C(x_2z_1) = 0.33$. The results also indicate that the correlative coherence of the two-population trajectories $\{X_1, X_2\}$ is two-to-three fold higher at moderate-to-high levels of niche overlap compared with the correlative coherence of the overall system $\{X_1, X_2, Z_1, Z_2\}$ when the noise is low and an order of magnitude lower at low levels of niche overlap when the noise is high. In this latter case, however, the coherence of the overall system arises from the coherence of the signals $\{X_1, Z_1\}$ and $\{X_2, Z_2\}$ rather than the signals $\{X_1, X_2\}$.

In summary, the results imply that for high levels of competition and low levels of noise (Fig. 4A), the coherence of system $\{X_1, X_2, Z_1, Z_2\}$ is less than system $\{X_1, X_2\}$ because the system coherence of $\{X_1, X_2, Z_1, Z_2\}$ arises primarily from competitive interactions between the populations. At moderate noise the system coherence of $\{X_1, X_2, Z_1, Z_2\}$ becomes evident at low competition levels (Fig. 4B) because the contribution of correlations between populations and resources to total system coherence is now stronger. Finally, at high noise

levels, the population–resource correlations now dominate low-to-moderate levels of competition, and also high levels of competition (Fig. 4C) because, in this latter case, the density of one of the population is strongly repressed through competition from the other.

The real power of CCA in teasing apart stochastic components of signals becomes more evident, however, with higher dimensional systems. For the three-population–three-resource system considered here, at low noise levels, the coherence of the total system $\{X_1, X_2, X_3, Z_1, Z_2, Z_3\}$ is similar to the coherence of the two most coherent subsystems, in this case $\{X_1, X_3, Z_1, Z_3\}$ and $\{X_2, X_3, Z_2, Z_3\}$. By contrast, at high noise levels the total system coherence is almost identical with the least coherent subsystem, in this case $\{X_1, X_3, Z_1, Z_3\}$ (not $\{X_1, X_2, Z_1, Z_2\}$ as symmetry might suggest!). This is a result that could not be predicted without a model. For this system, the correlative coherence $\mathrm{Cor}(x_1x_2x_3)$ of the system trajectories $\{X_1, X_2, X_3\}$ is not a reasonable indicator of the total correlative coherence $\mathrm{Cor}(x_1x_2x_3z_1z_2z_3)$. Generally, the total correlative coherence $\mathrm{Cor}(x_1x_2x_3z_1z_2z_3)$ is substantially less than the population-only correlative coherence $\mathrm{Cor}(x_1x_2x_3)$, except when the populations are specialists and noise levels are moderate to high or the populations are generalists and the noise is at its very highest level. These latter exceptions arise because, for these cases, the correlations between one or more of the state variables and one or more of the environmental variables are much higher than the correlations between any two state variables.

In a nutshell, at low levels of competition (Fig. 5A), the coherence of $\mathrm{Cor}(x_1x_2x_3z_1z_2z_3)$ is relatively low and only increases as resource variation increasingly entrains the different populations (cf. Figs. 2C–F, which correspond to the values $\gamma_1 = 7$, $\gamma_2 = 5$ and $\gamma_3 = 3$), except for the very highest noise levels. At intermediate and high competition levels the correlative coherence of the total system is dominated by competition processes involving the most stable subsystems (i.e. populations 2 and 3 with $\gamma_2 = 5$ and $\gamma_3 = 3$) rather than through entrainment of resource variation.

5. Conclusion

We expect population and environmental time series to be correlated when the latter influence the former in some way. Strong influences will produce large correlations. These correlations can be degraded by nonlinear processes intrinsic to population processes. Here I examined the effects of both intra and interspecific competition in degrading correlations in populations driven by noisy resources. Of course, other population processes—such as predation, time delays introduced because of aging (with the additional complication that different demographic parameters may be influenced by different environmental factors—cf. Higgins et al., 1997), or nonlinear dynamics influenced by spatial structure (cf. Hastings, 2001) are also bound to influence correlations between populations and noise in driving variables.

Correlations between pairs, as illustrated in the first part of the analysis, provide a basis for addressing the effects of population processes on the entrainment of environmental noise. CCA, however, allows us to move the analysis to a deeper level by generalizing the concept of correlation between two signals to the correlative coherence of n signals. Further, if the correlative coherence value, r, is regarded as a measure of the "systemness" of a system, then this measure can be used to compare the systemness of systems of different dimension. Ultimately, the real strength of CCA will be its application to sets of empirical data to determine the degree to which subsets of this data can be regarded as independent, or close to independent of one another. Also, one can envision numerically intensive, but automated, software being developed to hierarchically or categorically organize subsets of a set of n signals based on the degree of correlatively coherence of the various subsets.

In the future, automated software implementations of CCA—that is, calculating the correlative coherence (and associated standard errors) of a set of signals, and of selected subsets of that set—may become as ubiquitous and as useful as PCA (principle components analysis) is today. These two methods provide very different but complementary views of the same data in our quest to understand the degree to which a set of signals represents the output of a coherent system of interacting variables.

Acknowledgments

I thank Peter Baxter, Eran Karmon, James Lloyd-Smith, Jessica Redfern, Maria Sanchez and Chris Wilmers for comments that have improved this paper. This research was supported by NSF Grant DEB-0090323.

References

Beddington, J.R., 1975. Mutual interference between parasites or predators and its effect on searching efficiency. J. Anim. Ecol. 44, 331–340.

Bendat, J.S., Piersol, A.G., 1966. Measurement and Analysis of Random Data. Wiley, New York.

Bjornstad, O.N., Grenfell, B.T., 2001. Noisy clockwork: time series analysis of population fluctuations in animals. Science 293, 638–643.

Bjornstad, O.N., Sait, S.M., Steven, M., Stenseth, N.C., Thompson, D.J., Begon, M., 2001. The impact of specialized enemies on the dimensionality of host dynamics. Nature 409, 1001–1006.

Cencini, M., Falcioni, M., Olbrich, E., Kantz, H., Vulpiani, A., 2000. Chaos or noise: difficulties of a distinction. Phys. Rev. E 62, 427–437.

Cohen, J.E., 1995. Unexpected dominance of high frequencies in chaotic nonlinear population models. Nature 378, 610–612.

Cushing, J.M., Dennis, B., Desharnais, R.A., Costantino, R.F., 1998. Moving toward an unstable equilibrium: saddle nodes in population systems. J. Anim. Ecol. 67, 298–306.

Davies, P.I., Higham, N.J., 2000. Numerically stable generation of correlation matrices and their factors. BIT 40, 640–651.

DeAngelis, D.L., Goldstein, R.A., O'Neill, R.V., 1975. A model for trophic interaction. Ecology 56, 881–892.

Dennis, B., Desharnais, R.A., Cushing, J.M., Henson, S.M., Costantino, R.F., 2001. Estimating chaos and complex dynamics in an insect population. Ecol. Monogr. 71, 277–303.

Feigenbaum, M.J., 1980. The metric universal properties of period doubling bifurcations and the spectrum for a route to turbulence. Ann. N. Y. Acad. Sci. 357, 330–336.

Getz, W.M., 1984. Population dynamics: a per capita resource approach. J. Theor. Biol. 108, 623–644.

Getz, W.M., 1991. A unified approach to multispecies modeling. Nat. Resour. Modeling 5, 393–421.

Getz, W.M., 1993. Metaphysiological and evolutionary dynamics of populations exploiting constant and interactive resources: r-K selection revisited. Evol. Ecol. 7, 287–305.

Getz, W.M., 1994. A metaphysiological approach to modeling ecological populations and communities. In: Levin, S.A. (Ed.), Frontiers in Mathematical Biology. Springer, New York, pp. 411–442.

Getz, W.M., 1996. A hypothesis regarding the abruptness of density dependence and the growth rate of populations. Ecology 77, 2014–2026.

Getz, W.M., 2001. Competition, extinction, and sexuality of species. Ann. Zool. Fenn. 38, 315–330.

Hastings, A., 2001. Transient dynamics and persistence of ecological systems. Ecol. Lett. 4, 215–220.

Henson, S.M., Costantino, R.F., Cushing, J.M., Desharnais, R.A., Dennis, B., King, A.A., 2001. Lattice effects observed in chaotic dynamics of experimental populations. Science 294, 602–605.

Higgins, K., Hastings, A., Botsford, L.W., 1997. Density dependence and age structure: nonlinear dynamics and population behavior. Am. Nat. 149, 247–269.

Kaitala, V., Ylikarjula, J., Ranta, E., Lundberg, P., 1997. Population dynamics and the colour of environmental noise. Proc. R. Soc. London Ser. B: Biol. Sci. 264, 943–948.

May, R.M., 1974. Biological populations with nonoverlapping generations: stable points, stable cycles, and Chaos. Science 186, 645–647.

May, R.M., Oster, G.F., 1976. Bifurcations and dynamic complexity in simple ecological models. Am. Nat. 110, 573–590.

Morrison, D.F., 1976. Multivariate Statistical Methods, 3rd Edition. McGraw-Hill, New York, NY.

Noble, B., Daniel, J.W., 1977. Applied Linear Algebra. 2nd Edition. Prentice-Hall, Englewood Cliffs, NJ.

Ripa, J., Lundberg, P., Kaitala, V., 1998. A general theory of environmental noise in ecological food webs. Am. Nat. 151, 256–263.

Poon, C.-S., Barahona, M., 2001. Titration of chaos with added noise. Proc. Natl. Acad. Sci. (USA) 98, 7107–7112.

Schoombie, S.W., Getz, W.M., 1998. Evolutionary stable density-dependent strategies in a generalized Beverton and Holt model. Theor. Popul. Biol. 53, 216–235.

Shaffer, M.L., 1981. Minimum population sizes for species conservation. BioScience 31, 131–134.

Shannon, C., Weaver, W., 1949. The Mathematical Theory of Communication. University of Illinois Press, Urbana, IL.

Sugihara, G., May, R.M., 1990. Nonlinear forecasting as a way of distinguishing chaos from measurement error in time series. Nature (London) 344, 734–741.

Sugihara, G., Grenfell, B., May, R.M., 1990. Distinguishing error from chaos in ecological time series. Philos. Trans. R. Soc. London B: Biol. Sci. 330, 235–250.

Venables, W.N., Ripley, B.D., 1997. Modern Applied Statistics with S-Plus. 2nd Edition. Springer, New York, p. 548.